EXTENSIONAL FLOW OF NEMATIC LIQUID CRYSTAL UNDER ELECTRIC FIELD GRADIENT

L.J. CUMMINGS, J. LOW, AND T.G. MYERS

Abstract. Systematic asymptotic methods are used to formulate a model for the extensional flow of a thin sheet of nematic liquid crystal. With no external body forces applied, the model is found to be equivalent to the so-called Trouton model for Newtonian sheets (and fibers), albeit with a modified "Trouton ratio". However, with a symmetry-breaking electric field gradient applied, behavior deviates from the Newtonian case, and the sheet can undergo finite-time breakup if a suitable destabilizing field is applied. Some simple exact solutions are presented to illustrate the results in certain idealized limits, as well as sample numerical results to the full model equations.

1. Introduction

Nematic liquid crystals are ubiquitous in nature, and find wide application in many industrial processes. Many modern display devices, as well as other optical applications (including those in the cosmetics industry: many modern makeup products rely on liquid crystals for their iridescent optical qualities); certain thermometers, and some biopathogen detection methods are just a few examples where the liquid crystalline nature of the chemicals involved is key to performance [15]. An understanding of how liquid crystals behave under a wide variety of conditions is thus important; but due to the highly complex nature of the governing dynamic equations it can be very challenging to investigate behavior theoretically from a mechanistic viewpoint. Simple experimental setups can therefore be very valuable as an investigative tool to reveal novel behavior and new regimes not exhibited by Newtonian fluids. For example, a system as simple as a spreading nematic droplet can exhibit highly complex fingering instabilities [16]; an asymptotically-reduced mathematical model [1, 4, 5] reveals that these are probably due to the different boundary effects at the rigid substrate and the free surface.

In this paper we investigate another such simple experimental configuration that allows free-surface dynamics to be investigated using analytical tools: a two-dimensional "nematic liquid bridge", or nematic sheet. This scenario is very well understood for the Newtonian case (due to its wide application in, for example, a variety of glass manufacturing processes; see for example [10, 11] and references therein), but apart from some preliminary experimental studies on nematic fibers by Savage *et al.* [20], has not been studied in the nematic case. Here we employ

systematic asymptotic methods to derive a simplified mathematical model for the evolution of such a thin sheet. With certain simplifying assumptions a closed system of governing equations coupling the flow velocity of the nematic liquid crystal along the sheet's centerline, and the sheet thickness, can be obtained. The setup is similar to that of a drawn fiber (which was studied for the nematic case by Cheong & Rey [19]), but, due to the simpler geometry of the sheet (which makes dealing with the free surface anchoring conditions on the nematic molecules easier), the model we obtain is more tractable analytically. To explore the sheet dynamics more fully, we also consider its response to an applied electric field.

The paper is set out as follows: in section 2 we describe the modeling, the asymptotic approximations made to derive a simplified model; and give a brief discussion of suitable boundary conditions. Section 3 deals with simple explicit solutions of the reduced asymptotic model: first possible steady states in the presence of an electric field (and their stability characteristics) are considered; and second, it is shown that when surface tension effects are neglected the model may be solved exactly (special cases of such solutions are presented). The detailed analysis of electric field effects is relegated to an Appendix. In section 4 we carry out numerical simulations of the full unsteady model and explore dependence on initial and boundary conditions, and on electric field gradients. Finally, in section 5 we present our conclusions.

2. The model

The details of the theory governing the flow of NLCs are well documented and provided in texts such as [3, 8, 14]. The notation we employ is mostly the same as that used by Leslie [14], the two main functions being the velocity field of the flow, $\boldsymbol{v} = (v_1, v_2, v_3) = (u, v, w)$, and the director field $\boldsymbol{n}$, the unit vector describing the orientation of the anisotropic axis in the liquid crystal (an idealised representation of the local preferred average direction of the rod-like liquid crystal molecules). The evolution of $\boldsymbol{n}$ is determined by elastic stresses within the NLC, by the local flow-field, and by any externally-acting fields. In this paper we shall restrict attention to the 2D case in which flow, and the director field, are confined to the (x, z)-plane, so that $\boldsymbol{v} = (v_1, 0, v_3) = (u, 0, w)$, and $\boldsymbol{n} = (\sin\theta, 0, \cos\theta)$. We also neglect inertia from the outset, since only slowly-deforming sheets will be considered.

The governing equations holding in the bulk sample (allowing for the possibility of a dielectric effect due to an applied electric field $\boldsymbol{E}$, but neglecting inertial effects) are:

$$\frac{\partial}{\partial x_i}\left(\frac{\partial W}{\partial \theta_{x_i}}\right) - \frac{\partial W}{\partial \theta} + \tilde{g}_i \frac{\partial n_i}{\partial \theta}, \tag{1}$$

$$0 = -\frac{\partial \pi}{\partial x_i} + \tilde{g}_k \frac{\partial n_k}{\partial \theta} + \frac{\partial \tilde{t}_{ik}}{\partial x_k} \tag{2}$$

$$\frac{\partial v_i}{\partial x_i} = 0, \tag{3}$$

representing energy, momentum, and mass conservation, respectively. The quantities $\tilde{\boldsymbol{g}}$ and π are defined by

$$\tilde{g}_i = -\gamma_1 N_i - \gamma_2 e_{ik} n_k, \qquad e_{ij} = \frac{1}{2}\left(\frac{\partial v_i}{\partial x_j} + \frac{\partial v_j}{\partial x_i}\right), \tag{4}$$

$$N_i = \dot{n}_i - \omega_{ik} n_k, \qquad \omega_{ij} = \frac{1}{2}\left(\frac{\partial v_i}{\partial x_j} - \frac{\partial v_j}{\partial x_i}\right), \tag{5}$$

$$\pi = p + W, \tag{6}$$

where γ_1 and γ_2 are constants and p is the pressure; and W is the bulk energy, containing elastic and possible dielectric contributions. It is defined in terms of the director by

$$\begin{aligned} 2W = {} & K_1(\nabla \cdot \boldsymbol{n})^2 + K_2(\boldsymbol{n} \cdot \nabla \wedge \boldsymbol{n})^2 + K_3\big((\boldsymbol{n} \cdot \nabla)\boldsymbol{n}\big) \cdot \big((\boldsymbol{n} \cdot \nabla)\boldsymbol{n}\big) \\ & - \varepsilon\varepsilon_\perp \boldsymbol{E} \cdot \boldsymbol{E} - \varepsilon(\varepsilon_\parallel - \varepsilon_\perp)(\boldsymbol{n} \cdot \boldsymbol{E})^2, \end{aligned} \tag{7}$$

where K_1, K_2 and K_3 are elastic constants, ε is the permittivity of free space and $\varepsilon_\parallel$ and $\varepsilon_\perp$ are the relative dielectric permittivities parallel and perpendicular to the long axis of the molecules. Finally, $\tilde{t}_{ij}$ is the extra-stress tensor (related to the stress σ_{ij} by $\sigma_{ij} = -\pi\delta_{ij} + \tilde{t}_{ij}$), given by:

$$\tilde{t}_{ij} = \alpha_1 n_k n_p e_{kp} n_i n_j + \alpha_2 N_i n_j + \alpha_3 N_j n_i + \alpha_4 e_{ij} + \alpha_5 e_{ik} n_k n_j + \alpha_6 e_{jk} n_k n_i, \tag{8}$$

where the α_i are constant coefficients having the dimensions of viscosity though they are not necessarily positive (they are related to the γ_i in (4) by $\gamma_1 = \alpha_3 - \alpha_2$, $\gamma_2 = \alpha_6 - \alpha_5$), and $\mu = \alpha_4/2$ corresponds to the dynamic viscosity in the standard Newtonian (isotropic) case when all other α_i are zero.

Equation (1) is the energy equation, in which the terms in W represent the elastic energy associated with the director field; and the tendency of the director to align in an applied electric field $\boldsymbol{E}$ (when $\varepsilon_\parallel > \varepsilon_\perp$). The $\tilde{\boldsymbol{g}}$ term couples to the fluid flow. The three elastic contributions to the energy in (7) are known as splay, twist and bend, respectively, and represent energy penalties incurred when the director field has local behavior of these types [8].

The model must be solved subject to appropriate boundary conditions. For a stretched sheet with free surfaces these are: an anchoring condition on the director field at each of the free surfaces; a stress balance condition that equates the stress vector at each sheet surface to any external forces acting; and a kinematic condition at each sheet surface. Since any real sheet is of finite extent, we also include boundary conditions at the sheet's ends that specify how the sheet is being stretched (specified end velocities, and a constant pulling force, are the two driving scenarios considered here).

The anchoring condition models the fact that the molecules of the liquid crystal have a preferred orientation at a free interface, and is detailed below. The stress

balance takes the form

$$\boldsymbol{\sigma}\boldsymbol{\nu}^{\pm} = -\hat{\gamma}\kappa^{\pm}\boldsymbol{\nu}^{\pm} \quad \text{on } z = H \pm h/2, \tag{9}$$

where $\sigma_{ij} = -\pi\delta_{ij} + \tilde{t}_{ij}$ is the stress tensor, $\boldsymbol{\nu}^{\pm}$ is the outward normal vector to the free surface $z = H \pm h/2$, $\kappa^{\pm}$ is its curvature; and $\hat{\gamma}$ is a coefficient of surface tension. The kinematic condition states

$$\boldsymbol{v} \cdot \boldsymbol{\nu}^{\pm} = V_{\nu}^{\pm} \quad \text{on } z = H \pm h/2, \tag{10}$$

where $V_{\nu}^{\pm}$ is the outward normal velocity of the interface $z = H \pm h/2$.

2.1. **Scaling and nondimensionalisation.** The experimental set-up we have in mind is a thin 2D sheet of nematic liquid crystal (NLC), extended from its ends. The Newtonian analog has been considered by several authors; we will follow the approach of Howell [10, 11] (but see also van de Fliert, Howell & Ockendon [7] and the many references within these papers for other asymptotic work on the Newtonian problem).

We formulate the problem for the general case in which the NLC film occupies the region between the two free surfaces $z = H \pm h/2$, where $H(x,t)$ represents the centerline and $h(x,t)$ is the thickness. However, as in the Newtonian case it will emerge that the centerline is straight to leading-order for any sheet in extensional flow (at least on any relevant timescales).

To derive systematic asymptotic approximations to the governing equations we introduce appropriate scalings for the flow variables as follows [24]

$$(x,z) = L(\tilde{x}, \delta\tilde{z}), \quad (u,w) = U(\tilde{u}, \delta\tilde{w}), \quad t = \frac{L}{U}\tilde{t}, \quad \pi = \frac{\mu U}{L}\tilde{p},$$

where L is the lengthscale of typical variations in the x-direction (for example, it could be the initial length of the sheet); U is a typical flow velocity along the sheet axis (usually fixed by pulling on the sheet's ends); $\delta = \hat{h}/L \ll 1$ is a typical aspect ratio of the sheet ($\hat{h}$ being a typical sheet thickness), and $\mu \equiv \alpha_4/2$ is the representative viscosity scaling in the pressure (since this corresponds to the usual viscosity in the isotropic case in (8)).[1] We also write $h = \hat{h}\tilde{h}$, $H = \hat{h}\tilde{H}$ to define the dimensionless sheet width and centerline equation.

If $K = K_1$ is a representative value of the elastic constants K_1, K_2, K_3, (7) gives the appropriate scaling for W as

$$W = \frac{K}{\delta^2 L^2}\tilde{W},$$

assuming that elastic effects are important at leading order. Since the director field is a 2D unit vector we write it as

$$\boldsymbol{n} = (\sin\theta, 0, \cos\theta), \quad \theta(x,z,t). \tag{11}$$

[1]The coefficient α_4 is always positive, as may be shown by considering the entropy of the system [14].

We assume further that the elastic constants K_1 and K_3 are equal: $K_1 = K_3 = K$ (see *e.g.* [8, 22] for the validity of this commonly-used assumption), and that any applied electric field has a component only in the z-direction:

$$\boldsymbol{E} = a(x)\boldsymbol{e}_z + O(\delta), \tag{12}$$

(where $a(x)$ is, in principle, arbitrary; see Appendix B for the detailed justification of this electric field, which is the most general form compatible with Maxwell's equations and with no variation across the sheet). Then we write $a(x) = E_0\tilde{a}(\tilde{x})$ to nondimensionalize the electric field, where E_0 is some representative field strength.

Henceforth we drop the tildes, on the understanding that we are working in the dimensionless variables (unless explicitly stated otherwise).

2.2. **Asymptotic expansion of the governing equations.** In the dimensionless variables, but dropping the tildes, the bulk energy W in (7) is

$$W = \frac{1}{2}\left(\theta_z^2 + \delta^2\theta_x^2\right) - \delta e(x)\cos^2\theta - \delta\lambda e(x) \tag{13}$$

where

$$e(x) = \frac{\hat{h}LE_0^2 a(x)^2\varepsilon(\varepsilon_\parallel - \varepsilon_\perp)}{K} = e_0 a(x)^2, \quad \lambda = \frac{\varepsilon_\perp}{\varepsilon_\parallel - \varepsilon_\perp}, \tag{14}$$

and thus, for example, $e(x)$ is quadratic in x if $a(x)$ is linear in x. Here we assume that e, e_0, a are order-one, so that elasticity is the dominant contribution to the bulk energy; however, we allow the electric field effect to be comparable to the surface energy, as we now explain.

The director field satisfies "anchoring" boundary conditions at each surface, which model its tendency to align at a certain angle, θ_B, with the normal to the interface $\boldsymbol{\nu}$ (in the absence of external forces, θ_B is the angle that minimizes surface energy for the system). Since both interfaces are free and assumed to be in contact with air we take θ_B to be the same angle for each surface (though it is possible that different conditions could be manufactured for the two surfaces, for example, if the sheet is a barrier between two different gases). We take an *ad-hoc* anchoring condition which says that, in the absence of an applied field, the director will take the preferred direction; but that an applied field will act to pull the anchoring angle towards the field direction (z-direction, within the sheet):

$$\theta = \theta_B g(a(x)) \quad \text{on } z = H \pm h/2. \tag{15}$$

The function g is monotonically decreasing in a and tends to zero for large a to align the director fully with the field. One possible form, which is the form we will assume for all of our example calculations in this paper, is

$$g(a) = \frac{E_a^\alpha}{a^\alpha + E_a^\alpha}, \tag{16}$$

for some parameters $E_a > 0$ (an alignment field strength) and $\alpha > 1$. This anchoring condition is only approximate, since in the absence of a field θ assumes the value θ_B, whereas it should be the angle between $\boldsymbol{n}$ and ν that takes the value θ_B. However, in our asymptotic approximation $\nu = \pm(0,1) + O(\delta^2)$, so that the condition (15) is correct to the order required.

We asymptotically expand all dependent variables (θ, u, v, p, H, h) in powers of the small parameter $\delta = \hat{h}/L$, and substitute into equations (1)–(3) to obtain a hierarchy of governing equations at orders 1, δ, δ^2, etc. The boundary conditions (9), (10) and (15) are Taylor-expanded onto the leading-order free boundaries $z = H_0 \pm h_0/2$ to yield boundary conditions for the governing equations at each order in δ. The x- and z-components of the momentum equations (2) and the energy equation (1) at leading order then reduce to

$$u_{0zz}\big(\alpha_4 - (\alpha_2 - \alpha_5)\cos^2\theta_0 + (\alpha_3 + \alpha_6)\sin^2\theta_0 + 2\alpha_1 \sin^2\theta_0 \cos^2\theta_0\big) + \\ +2u_{0z}\theta_{0z}\big(\alpha_2 + \alpha_3 - \alpha_5 + \alpha_6 + 2\alpha_1\cos 2\theta_0\big)\sin\theta_0\cos\theta_0 = 0, \tag{17}$$

$$u_{0zz}\big(\alpha_1 + \alpha_2 + \alpha_3 + \alpha_5 + \alpha_6 + \alpha_1\cos 2\theta_0\big)\sin\theta_0\cos\theta_0\big) - 2\hat{N}\theta_{0zz}\theta_{0z} + \\ +u_{0z}\theta_{0z}\big(\alpha_1\cos 4\theta_0 + (\alpha_1 + \alpha_2 + \alpha_3 + 2\alpha_5)\cos 2\theta_0 - \alpha_2 + \alpha_3\big) = 0, \tag{18}$$

$$2\hat{N}\theta_{0zz} - u_{0z}\big(\alpha_2 - \alpha_3 + (\alpha_6 - \alpha_5)\cos 2\theta_0\big) = 0, \tag{19}$$

respectively, where the dimensionless parameter $\hat{N} = K/(\mu U \delta L)$ (an inverse Ericksen number) measures the relative importance of elastic and viscous effects. These equations must be solved subject to the leading-order boundary conditions at $z = H_0 \pm h_0/2$. The normal components of the stress conditions (9) at each interface yield, at order δ^{-1},

$$u_{0z} = 0 \quad \text{on } z = H_0 \pm h_0/2. \tag{20}$$

The leading order in the anchoring conditions (15) gives

$$\theta_0 = \theta_B g(a(x)) \quad \text{on } z = H_0 \pm h_0/2, \tag{21}$$

while the kinematic conditions (10) give

$$w_0 = H_{0t} + u_0 H_{0x} \pm \frac{1}{2}(h_{0t} + u_0 h_{0x}) \quad \text{on } z = H_0 \pm h_0/2. \tag{22}$$

Eliminating u_{0z} between equations (18) and (19) reveals θ_{0z} is constant and hence $u_{0z} = 0$. Applying the boundary conditions then determines

$$u_0 = u_0(x,t), \qquad \theta_0 = \theta_0(x) = \theta_B g(a(x)), \tag{23}$$

with g given by (16) (or similar). The leading-order incompressibility equation (3) may now be integrated to give an expression for w_0,

$$w_0 = H_{0t} + (u_0 H_0)_x - z u_{0x}, \tag{24}$$

where we have applied a kinematic condition (22) at the top surface. Applying the condition at the bottom surface provides the mass balance

$$h_{0t} + (u_0 h_0)_x = 0\,. \tag{25}$$

To make further progress we need to examine higher orders in the governing equations. At order δ in the x- and z-components of (2) we find

$$u_{1zz} = 0, \tag{26}$$

$$p_{0z} = 0, \tag{27}$$

where (26) was used to obtain (27). Hence $p_0 = p_0(x)$. The $O(\delta)$ energy equation (1) gives

$$\begin{aligned} u_{0x}(\alpha_5 - \alpha_6)\sin 2\theta_0 + \frac{1}{2}\big(\alpha_3 - \alpha_2 + (\alpha_5 - \alpha_6)\cos 2\theta_0\big)u_{1z} \\ + \hat{N}\big(\theta_{1zz} - e(x)\sin 2\theta_0\big) = 0. \end{aligned} \tag{28}$$

This last equation will give θ_1 in terms of u_0, θ_0.

We now require the boundary conditions at the appropriate order. The $O(1)$ normal component of the stress conditions (9) gives

$$\begin{aligned} u_{1z} &= \frac{u_{0x}(\alpha_6 - \alpha_5 + \alpha_1\cos 2\theta_0)\sin 2\theta_0}{\alpha_4 - (\alpha_2 - \alpha_5)\cos^2\theta_0 + (\alpha_3 + \alpha_6)\sin^2\theta_0 + 2\alpha_1\sin^2\theta_0\cos^2\theta_0} \\ &\equiv U_1(\theta_0)u_{0x}\,, \end{aligned} \tag{29}$$

on $z = \pm\frac{h_0}{2}$. Combining equations (26) and (29) gives

$$u_1 = zU_1(\theta_0)u_{0x} + U_0(x,t), \tag{30}$$

where U_0 is undetermined and U_1 is defined in (29). The $O(1)$ tangential components of the stress conditions (9) give the same result on both upper and lower free boundaries, $z = \pm h_0/2$,

$$\begin{aligned} p_0(x,t) = &-(\alpha_4 + (\alpha_5 + \alpha_6 + \alpha_1\cos 2\theta_0)\cos^2\theta_0)u_{0x} + \\ &+ \frac{u_{0x}U_1(\theta_0)}{2}(\alpha_1 + \alpha_2 + \alpha_3 + \alpha_5 + \alpha_6 + \alpha_1\cos 2\theta_0)\sin\theta_0\cos\theta_0 - \frac{\gamma}{2}h_{0xx} \end{aligned} \tag{31}$$

where $\gamma = \hat{\gamma}\delta/(\mu U)$ is a dimensionless coefficient of interfacial tension. Since the condition takes the same form on both free boundaries, and contains only functions that are independent of z, in fact the right-hand side must give the expression for the leading-order pressure throughout the sheet.

Returning to equation (28) above, we can now solve for θ_1 after applying the appropriate anchoring condition at $O(\delta)$, $\theta_1 = 0$ on $z = \pm h_0/2$. The problem reduces to

$$\begin{aligned} \theta_{1zz} = &\, e(x)\sin 2\theta_0 \\ &- \frac{u_{0x}}{\hat{N}}\left[(\alpha_5 - \alpha_6)\sin 2\theta_0 + \frac{U_1(\theta_0)}{2}\big(\alpha_3 - \alpha_2 + (\alpha_5 - \alpha_6)\cos 2\theta_0\big)\right] \end{aligned} \tag{32}$$

$$\equiv Q_1(x) \tag{33}$$

(here $Q_1(x)$ is introduced as convenient shorthand for the right-hand side of (32)). Hence we determine the unique solution

$$\theta_1 = \frac{Q_1(x)}{2}\left(z^2 - \frac{h_0(x,t)^2}{4}\right). \tag{34}$$

We now have expressions for θ_0, θ_1, p_0 and a mass balance relating the unknowns u_0, h_0. To close the system we must continue to yet higher orders. The algebra now becomes too cumbersome to describe in detail: it involves examining equation (2) to $O(\delta^2)$, which leads to an equation for u_{2zz}. Integration then leads to

$$u_{2z}|_{z=h_0/2} - u_{2z}|_{z=-h_0/2} = \int_{-h_0/2}^{h_0/2} u_{2zz}\, dz = h_0 K(x,t)\,, \tag{35}$$

where K is known in terms of u_0, θ_0. The terms u_{2z} evaluated on both free boundaries are given by the stress conditions (9) at $O(\delta)$. So, finally, we obtain an extra equation relating u_0 and h_0, which can be solved, together with (25), to yield the leading order solution.

We examine the cases with and without an electric field separately below. Since we have now reduced the problem to one for leading-order dependent variables u_0, h_0, θ_0, we drop the subscripts on these quantities.

2.2.1. *No electric field, $a(x) = 0 = e(x)$.* With no electric field the leading order director angle θ is simply constant (see (23)), dictated by anchoring conditions, and we may set it to zero with no loss of generality (the solvability condition (35) above is somewhat messy for a general value of θ (see equation (71) in Appendix A), but in all cases takes the same general form). For $\theta = 0$ we obtain

$$\big(2\alpha_4 + \alpha_1 + \alpha_5 + \alpha_6\big)\big(u_x h\big)_x + \frac{\gamma}{2} h h_{xxx} = 0, \tag{36}$$

which must be solved together with equation (25),

$$h_t + (uh)_x = 0. \tag{37}$$

The governing equations for a Newtonian film are retrieved by setting $\alpha_1 = \alpha_2 = \alpha_3 = \alpha_5 = \alpha_6 = 0$ and $\alpha_4 = 1$. In general then the above equations are equivalent to the Newtonian case, with a difference only of timescale. The first term in (36) is the axial gradient of the (leading order) dimensionless tension in the sheet, and the premultiplying factor is known as the Trouton ratio. The Newtonian limit of equations (36) and (37) with surface tension $\gamma = 0$ is known as the Trouton model for a viscous sheet, and was considered in detail by Howell [10, 11] (see also references therein for earlier work on similar systems).

Appropriate boundary and initial conditions for equations (36) and (37) are that the initial profile of the sheet, $h_i(x) = h(x,0)$, is specified, and that we apply conditions at each end of the sheet. We consider a sheet stretched between

two plates that are pulled apart. We assume that one plate (one end of the sheet) is fixed: $u(0,t) = 0$, while the other, at $x = s(t)$, is pulled either with (a) prescribed velocity, or (b) prescribed force F. In case (a) the appropriate condition is $u(s(t),t) = \dot{s}(t)$, with $s(t)$ given (this is equivalent to specifying the position of the sheet's end); and in case (b) we have $F = h(s(t),t)(-p(s(t),t) + 2u_x(s(t),t))$, where F is prescribed but $s(t)$ is unknown. With $\gamma = 0$ these conditions suffice to close the problem; but if $\gamma \neq 0$ then we need an extra condition at each end, such as specification of the contact angle $\partial h/\partial x$ between the fluid and the plate. The boundary conditions are discussed further when solutions are presented in §3.

Since, to this order in the asymptotics, the behavior is essentially Newtonian in this field-free case, and this was considered exhaustively by Howell and co-authors [10,11], we move on to the more complicated model that results when an electric field is applied.

2.3. **Applied electric field.** The analog of equation (36) is extremely complicated with an applied field, and in the most general case it is not clear whether it ought to simplify significantly. However, since with no applied field we obtain essentially the Newtonian result, we are encouraged to examine the special case $\alpha_1 = \alpha_2 = \alpha_3 = \alpha_5 = \alpha_6 = 0$ to make further progress, and to determine the general form of the final governing equation in this situation. The appropriate governing equations are now equation (37):

$$h_t + (uh)_x = 0. \tag{38}$$

and

$$2\alpha_4\big(u_x h\big)_x + \hat{N}h\big(e(x)(\cos^2\theta + \lambda)\big)_x + \frac{\gamma}{2}hh_{xxx} = 0, \tag{39}$$

where $e(x)$ and λ are as defined in (14):

$$e(x) = \frac{\hat{h}LE_0^2 a(x)^2 \varepsilon(\varepsilon_\parallel - \varepsilon_\perp)}{K} = e_0 a(x)^2, \quad \lambda = \frac{\varepsilon_\perp}{\varepsilon_\parallel - \varepsilon_\perp}, \tag{40}$$

and the director angle θ is prescribed by (23b) and (16):

$$\theta_0(x) = \theta_B g(a(x)), \quad \text{with} \quad g(a) = \frac{E_a^\alpha}{a^\alpha + E_a^\alpha}, \tag{41}$$

where θ_B is the anchoring angle. The function $a(x)$ is determined by knowledge of the applied electric field (see Appendix B). The problem once again reduces to solving (38), (41) for u, h. In the following sections we consider various approaches to solving this model.

3. Simple model solutions

We first consider some simple exact solutions of our model: (i) steady state, achievable (in a nontrivial sense) only for the fixed-force end condition and with

nonzero surface tension γ; and (ii) exact unsteady "pulling" solutions, where the end velocity is prescribed, but surface tension is zero. These solutions, which we present only for simple choices of electric field, can act as a guide for more general numerical solutions, which we present later in §4.

We note that, for the steady solutions considered below, and for our subsequent numerical results, it is convenient to work on a fixed length domain, $[0, 1]$. We can re-scale by choosing $\xi = x/s(t)$, where $x = s(t)$ is the right-hand end of the sheet, so that the domain in ξ-space is the interval $[0, 1]$. Then the governing equations are

$$2s\alpha_4(u_\xi h)_\xi + \hat{N}hs^2\left[e(\xi)(\cos^2\theta + \lambda)\right]_\xi + \frac{\gamma}{2}hh_{\xi\xi\xi} = 0 \tag{42}$$

$$sh_t - \xi s_t h_\xi + (uh)_\xi = 0 \tag{43}$$

together with our definition for θ, (23b), (16).

When the velocities of the sheet ends are specified, appropriate boundary and initial conditions are

$$u(0,t) = 0, \qquad u(s(t),t) = \dot{s}(t), \qquad h(\xi,0) = h_i(\xi) \tag{44}$$

$$h_\xi(0,t) = -s\cot\phi_0 = -s\beta_0 \qquad\qquad h_\xi(1,t) = s\cot\phi_1 = s\beta_1\,, \tag{45}$$

where $s(t)$ is prescribed (and in the time-dependent case, we suppose $s(0) = 1$ for definiteness), and ϕ_0, ϕ_1 are contact angles at $x = 0$, $x = s(t)$. These angles are specified when $\gamma \neq 0$; if surface tension is neglected we only require the first set of conditions (44). If motion is driven by a specified force applied at one end of the bridge, an extra condition is required since the domain length $s(t)$ in x-space is unknown. This condition is an explicit conservation of mass constraint, which was automatically enforced by the previous boundary conditions (44). The force condition at the pulling end is

$$F = h(-p + 2u_x) \quad \text{at } x = s(t), \tag{46}$$

and thus the boundary conditions (44) are replaced by

$$u(0,t) = 0, \qquad F = h\left[\frac{f(\theta)}{s}u_\xi + \frac{\gamma}{2s^2}h_{\xi\xi} + \frac{2}{s}u_\xi\right]_{\xi=1}, \tag{47}$$

$$V = s\int_0^1 h\,d\xi, \tag{48}$$

where $f(\theta)$ here is the coefficient of $(-u_x)$ in the expression for the pressure (31). The position of the right hand boundary is defined by

$$s_t = u(1,t) \qquad s(0) = 1\,. \tag{49}$$

3.1. **Steady states.** With a prescribed (nonzero) velocity at the ends there is clearly no steady state; however, with a prescribed force a steady state is possible. Using the formulation above, the mass balance (43) shows that uh is constant,

and since $u(0,t)=0$ we infer that $u=0$ everywhere. Setting $u=0$ in (42), the problem is then governed by

$$\hat{N}s^2\left[e(\xi)(\cos^2\theta+\lambda)\right]_\xi+\frac{\gamma}{2}h_{\xi\xi\xi}=0. \tag{50}$$

In the absence of an electric field the film thickness is quadratic, with coefficients determined by conditions (45), (47)

$$h=\frac{s}{2}(\beta_1+\beta_0)\xi^2-s\beta_0\xi+\frac{2sF}{\gamma(\beta_0+\beta_1)}+\frac{s}{2}(\beta_0-\beta_1), \tag{51}$$

where the β_i are related to the contact angles; see (45). The position s of the sheet's right-hand end is then fixed by the volume condition (48) as

$$s^2=V\left[\frac{2F}{\gamma(\beta_0+\beta_1)}+\frac{1}{6}(\beta_0-2\beta_1)\right]^{-1}, \tag{52}$$

which simplifies to

$$s^2=\frac{6\gamma V\beta_0}{6F-\gamma\beta_0^2} \tag{53}$$

when the contact angles are equal ($\beta_1=\beta_0$). This result seems counterintuitive at first, since it says that a greater force corresponds to a shorter bridge, while smaller forces support longer bridges. However, it makes sense, since the surface tension force that must be countered is higher in a short, more highly-curved bridge, while a longer bridge is flatter and easier to sustain. A sufficiently large force applied to a short bridge would indeed elongate it; but if the force were sustained at the same high level then the bridge would elongate indefinitely and no steady state could be achieved. Note that there is a minimum threshold force for a steady state to exist, but any force $F>\gamma\beta_0^2/6$ gives rise to a steady state. Any "pushing" force $F<0$ acting to compress the sheet can never, of course, yield a steady state.

With an electric field equation (50) integrates once immediately, but then the remaining integration depends on the form of the field. In the simplest nontrivial case, where the term $[e(x)(\cos^2\theta+\lambda)]$ is linear in x, say

$$E_F=\hat{N}\left[e(x)(\cos^2\theta+\lambda)\right]_x, \tag{54}$$

for constant E_F, then

$$\begin{aligned}h=&-\frac{E_Fs^3\xi^3}{3\gamma}+\left[(\beta_0+\beta_1)+\frac{s^2E_F}{\gamma}\right]\frac{s\xi^2}{2}-\beta_0s\xi+\frac{2sF}{\gamma(\beta_0+\beta_1)-s^2E_F}-\\&-\frac{s^3E_F}{6\gamma}+\frac{s}{2}(\beta_0-\beta_1).\end{aligned} \tag{55}$$

The position s of the sheet's end is again determined by (48), which leads to a cubic equation for $y = s^2$:

$$(E_F y - \gamma(\beta_0 + \beta_1)) \left[V - \frac{y}{12} \left(2(\beta_0 - 2\beta_1) - \frac{E_F y}{\gamma} \right) \right] + 2Fy = 0. \tag{56}$$

The requirement that $y > 0$ for a given field E_F restricts the possible values for F; or vice-versa, if one thinks of specifying F and finding the field E_F that gives a steady solution. In particular, we see that for the right electric field, a steady state can exist even with zero force $F = 0$. In this case (setting $\beta_1 = \beta_0$ for simplicity),

$$y = -\frac{\gamma\beta_0}{E_F} \pm \sqrt{\frac{\gamma^2\beta_0^2}{E_F^2} - \frac{12\gamma V}{E_F}},$$

and while both solutions are negative for $E_F > 0$, one is positive for $E_F < 0$. For such solutions, the film thickness h is always zero at the pulling end $x = s$, as may be seen from condition (46). Note that the requirement that the film thickness $h \geq 0$ everywhere is not guaranteed, and solutions must be checked for this property, as well as for positive sheet length.

At large fields $|E_F| \gg 1$ solutions are possible only for $E_F > 0$. In this case an asymptotic expansion can be constructed for $y = s^2$, in inverse powers of E_F, and is found to yield

$$s^2 = \frac{\gamma(\beta_0 + \beta_1)}{E_F} \left[1 - \frac{2F}{VE_F} + O\left(\frac{1}{E_F^2} \right) \right],$$

$$h = s \left[-\frac{1}{3}(\beta_0 + \beta_1)\xi^3 + (\beta_0 + \beta_1)\xi^2 - \beta_0\xi - \frac{1}{3}(2\beta_1 - \beta_0) + \frac{VE_F}{\gamma(\beta_0 + \beta_1)} + O\left(\frac{1}{E_F} \right) \right]$$

provided $F \neq 0$ (this solution, which simplifies considerably for equal contact angles $\beta_1 = \beta_0$, is valid for both extensional and compressive forces F, as long as $|F| \ll E_F$). If the applied force F is large then it must be positive for solutions to exist, and when $F \gg 1$ the asymptotic solution for $y = s^2$ in inverse powers of F takes the form

$$s^2 = \frac{\gamma V}{2F}(\beta_0 + \beta_1) \left[1 - \frac{1}{12F}\big(\gamma(\beta_0 + \beta_1)(\beta_0 - 2\beta_1) + 6E_F V\big) + O\left(\frac{1}{F^2} \right) \right]$$

(this solution is valid for fields E_F of either sign, as long as $|E_F| \ll F$). The profile h depends on ξ only at order $1/\sqrt{F}$; at leading order (order F) and order-one h is constant,

$$h = \frac{2sF}{\gamma(\beta_0 + \beta_1)} \left(1 + \frac{E_F V}{2F} + O(F^{-3/2}) \right).$$

Several solutions, which illustrate the range of possibilities, are shown in figure 1. In all cases $\beta_0 = \beta_1 = 0.5$, which gives positive curvature, and $\gamma = 1 = V$. A negative value for E_F augments the surface tension force and so allows longer bridges; a positive value requires shorter bridges. If we choose $\beta_0 = \beta_1 < 0$ there is no real solution for s; no steady state of this kind exists, and presumably this form of bridge would rupture, likely at its end(s).

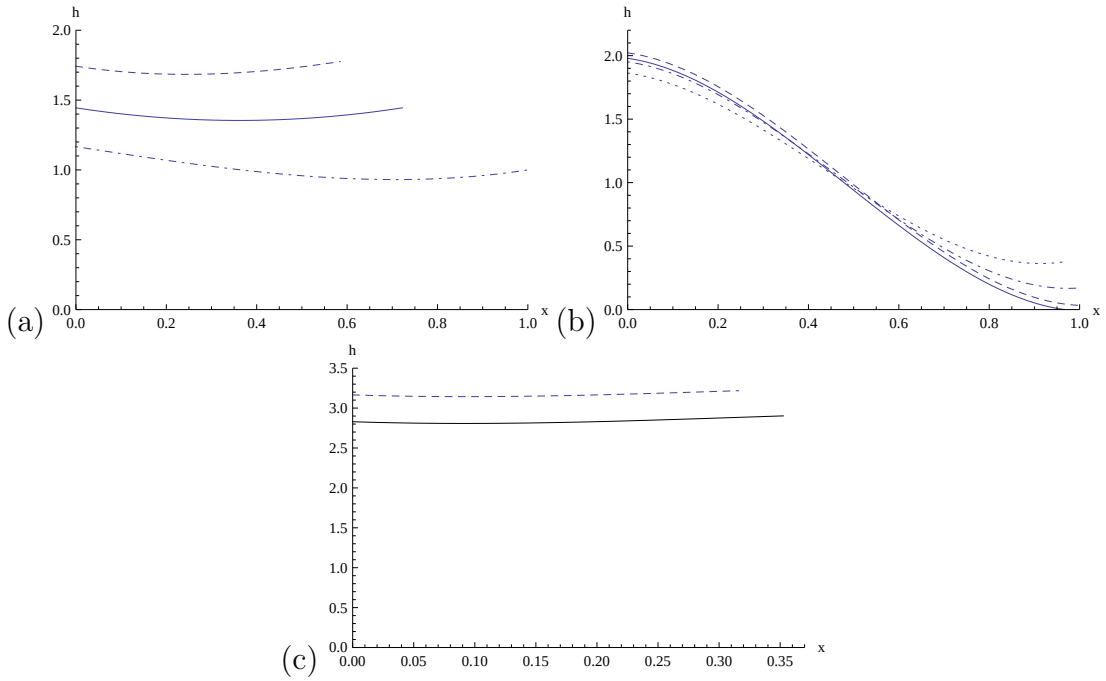

FIGURE 1. Solutions to the steady state problem with a constant force applied at one end. (a) Applied force is $F = 1$, while the field values are: $E_F = 1$ (dashed), $E_F = 0$ (solid) and $E_F = -1$ (dash-dotted). (b) Applied field is such that $E_F = -10$, while the force at the end is: $F = 0$ (solid), $F = 0.25$ (dashed), $F = 1$ (dash-dotted), and $F = 2$ (dotted). (c) Applied field is such that $E_F = 10$, while the force at the end is: $F = 0.01$ (dashed), $F = -1$ (solid).

3.2. **Solution of the zero surface tension model, $\gamma = 0$.** We now consider the case in which surface tension is negligible in the model, setting $\gamma = 0$ in the model (38)–(41) summarized in §2.3. Following the approach of Howell [10, 11] for Newtonian sheets, this model may be solved, at least in certain special cases, by introducing a Lagrangian transformation $(x, t) \mapsto (\eta, \tau)$, where

$$x_\tau = u(x(\eta, \tau), \tau), \quad x(\eta, 0) = \eta, \quad t = \tau. \tag{57}$$

Then

$$\partial_\tau = \partial_t + u\partial_x, \quad \text{and} \quad u_\eta = u_x x_\eta,$$

so that (37) becomes

$$h_\tau + \frac{hu_\eta}{x_\eta} = 0. \tag{58}$$

Now note that $u = x_\tau$, so $u_\eta = x_{\eta\tau}$, and (58) becomes

$$h_\tau x_\eta + h x_{\eta\tau} = (hx_\eta)_\tau = 0 \quad \Longrightarrow \quad x_\eta = \frac{h_i(\eta)}{h(\eta,\tau)}, \tag{59}$$

where $h_i(\eta) = h(\eta, 0)$ is the initial condition on the sheet profile.

In equation (39) we write

$$R(x) = \big(e(x)(\cos^2\theta + \lambda)\big)_x. \tag{60}$$

We will consider $R(x)$ to be a specifiable function, since $e(x) = e_0 a(x)^2$, $\theta = g(a(x))$ is a given function of $a(x)$, and we suppose the external electric field may be chosen so as to generate any form of $a(x)$ (how to calculate the required external field is described in Appendix B; note however that many choices of $a(x)$ will require an external field that may be very difficult or impossible to generate in practice). Writing the first term in (39) as $-2\alpha_4(h_\tau)_x$, and using (59), equation (39) (with $\gamma = 0$) becomes

$$\frac{4h_{\eta\tau}}{x_\eta} = \hat{N}Rh \quad \Longrightarrow \quad 4h_{\eta\tau} = \hat{N}R(\eta)h_i(\eta), \tag{61}$$

where R is as defined in (60) above. The system is closed by suitable boundary conditions as already discussed; with zero surface tension it is sufficient to specify the positions of the sheet's ends, or fix one end and specify the force applied to the other end. In the former case it is easy to integrate twice to find the explicit solution parametrically:

$$h(\eta,\tau) = A(\tau) + h_i(\eta) + \frac{\tau\hat{N}}{4}\int_0^\eta R(\eta')h_i(\eta')\,d\eta', \tag{62}$$

where h_i is the initial condition on the sheet thickness, $h(\eta, 0) = h_i(\eta)$ and $A(\tau)$ is fixed by specifying the sheet length $s(\tau)$, with $A(0) = 0$:

$$s(\tau) = \int_0^1 x_\eta d\eta = \int_0^1 \frac{h_i(\eta)\,d\eta}{A(\tau) + h_i(\eta) + \frac{\tau\hat{N}}{4}\int_0^\eta R(\eta')h_i(\eta')d\eta'}. \tag{63}$$

For physically-relevant solutions we assume $s(\tau)$ is a prescribed, increasing function of τ, with $s(0) = 1$.

The latter condition of a prescribed force at the sheet's end leads to a more complicated free boundary problem, and the exact solution cannot be obtained so neatly. We do not consider this case further analytically.

3.2.1. *Specific solution family: Rh_i constant.* The simplest nontrivial case to consider is when the combination Rh_i is constant (e.g. constant R and an initially flat sheet). Since $h_i > 0$ necessarily, R is then of one sign for all relevant η, so with no loss of generality we write $R(\eta)h_i(\eta) = \mathrm{sgn}(R)$, and explicitly evaluate the integral in (62) to give

$$h(\eta,\tau) = A(\tau) + h_i(\eta) + \mathrm{sgn}(R)\frac{\hat{N}\eta\tau}{4}. \tag{64}$$

To determine $A(\tau)$ then requires that we evaluate the integral in (63),

$$s(\tau) = \int_0^1 \frac{h_i(\eta)\,d\eta}{A(\tau) + h_i(\eta) + \mathrm{sgn}(R)\frac{\hat{N}\eta\tau}{4}} = \int_0^1 \frac{d\eta}{1 + |R|\left(A(\tau) + \mathrm{sgn}(R)\frac{\hat{N}\eta\tau}{4}\right)}, \tag{65}$$

which requires specification of h_i or R, and the pulling function $s(\tau)$.

For the particular case in which both h_i and R are constant ($h_i(\eta) = 1$, $R(\eta) = \mathrm{sgn}(R)$) we can evaluate $A(\tau)$ explicitly, and also invert the relation (59) to find $x(\eta,\tau)$, obtaining the exact solution parametrically as

$$h(\eta,\tau) = \frac{\mathrm{sgn}(R)\hat{N}\eta\tau}{4} + \frac{\mathrm{sgn}(R)\hat{N}\tau}{4(\exp(\frac{\hat{N}\eta\tau}{4}s(\tau)) - 1)},$$

$$x(\eta,\tau) = \frac{4}{\mathrm{sgn}(R)\hat{N}\tau}\log\left[\eta\left(\exp\left(\frac{\mathrm{sgn}(R)\hat{N}\tau}{4}s(\tau)\right) - 1\right) + 1\right].$$

For any monotone increasing pulling function $s(\tau)$ (assuming $s(\tau) < \infty$ while $\tau < \infty$) these solutions thin indefinitely at the ends (for both $\mathrm{sgn}(R) > 0, < 0$), but do not break off in finite time. Typical solutions are shown in figures 2 and 3.

By way of contrast we note that the equivalent Newtonian solution for $h_i(\eta) = 1$

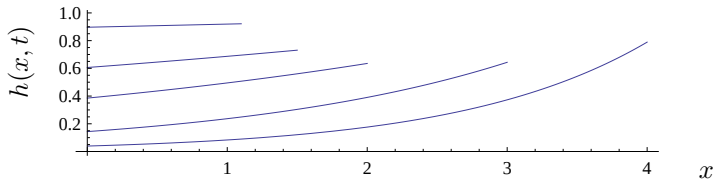

FIGURE 2. Exact solution to the unsteady problem for an initially-uniform sheet $h_i(x,0) = 1$, with the right-hand end pulled at unit speed so that its position is at $s(t) = 1+t$. The sheet profile is shown at times $t = 0.1, 0.5, 1, 2, 3$. The applied field is such that $R(x) = 1$ (as defined in (60)), and the parameter $\hat{N} = 1$.

is simply

$$h(\eta,\tau) = \frac{1}{s(\tau)}, \quad x = \eta s(\tau) \tag{66}$$

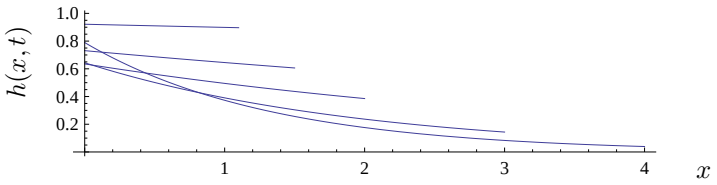

FIGURE 3. Exact solution to the unsteady problem for an initially-uniform sheet $h_i(x,0) = 1$, with the right-hand end pulled at unit speed so that its position is at $s(t) = 1+t$. The sheet profile is shown at times $t = 0.1, 0.5, 1, 2, 3$. The applied field is such that $R(x) = -1$ (as defined in (60)), and the parameter $\hat{N} = 1$.

(set $\hat{N} = 0$ in (62), (63) and (59)), so the Newtonian sheet is unaffected by the applied field and simply thins uniformly to conserve mass.

We can analyze the general solution (62) and show that for most choices of initial condition, any choice of pulling function $s(\tau)$ for which s becomes arbitrarily large will lead ultimately to film breakup. However, we cannot say with certainty where the film will break. So far in simulations film breakup has only been observed at the endpoints – whether or not internal breakup can occur is an open mathematical question.

4. Numerical solutions of the full model

We now present some numerical solutions of the full (time-dependent, nonzero surface tension) model equations, which numerically we solve in the fixed-domain form (42)–(43).

The first example we consider is the nonzero surface tension analog of the exact solution of §3.2.1. Again, we take the electric field to be such that $R(x) = \pm 1$, as defined in (60), and fix one end $x = 0$ of the initially uniform sheet ($h_i(x) = 1$), while the other end at $x = s(t)$ is pulled at unit speed, so that $u(s(t), t) = 1$, with $s(t) = 1 + t$ (c.f. (44)). This form of the electric field is particularly simple to implement, since the governing equation (42) reduces to

$$2s(u_\xi h)_\xi \pm \hat{N} h s^3 + \frac{\gamma}{2} h h_{\xi\xi\xi} = 0, \tag{67}$$

(recall we set $\alpha_4 = 1$ throughout). Since we include surface tension effects we must also specify the contact angles at the sheet's ends, as in (45). For an initially-flat sheet we choose contact angles of $\pi/2$ ($\beta_0 = 0 = \beta_1$), since these are compatible with the initial condition. The resulting numerical solutions are shown in figure 4, in which the left-hand figure with $R(x) = 1$ may be directly compared with figure 2, and the right-hand figure with $R(x) = -1$ may be compared with 3. The parameter $\hat{N} = 1$ in all cases, and results for surface tension parameter values $\gamma = 1$ (solid curves), and $\gamma = 4$ (dashed curves) are shown. The sheet profile is shown at times $t = 0.1, 0.5, 1, 2, 3$ as it extends.

Different contact angles are explored by means of a different initial condition,

$$h_i(\xi, 0) = c\cosh([\xi - 0.5]/c) - c\cosh(0.5/c) + 1, \tag{68}$$

with $c = 1.039$ to match boundary conditions $\beta_0 = \beta_1 = 0.5$. Simulations for this initial condition are shown in figure 5 (again, the left-hand subfigure has $R(x) = 1$ while $R(x) = -1$ in the right-hand subfigure). Here the contact angles at the sheet's ends are specified by setting $\beta_0 = \beta_1 = 0.5$. The sheet's right-hand end is pulled at unit speed, the parameter $\hat{N} = 1$, and results for two surface tension values $\gamma = 1$ (solid curves), and $\gamma = 4$ (dashed curves) are shown. The evolution is shown over longer times here (up to $t = 4$ in the left-hand figure and up to $t = 6$ in the right-hand figure) to give a qualitative feel for the large-time evolution of such a sheet. While the behavior is qualitatively similar in zero

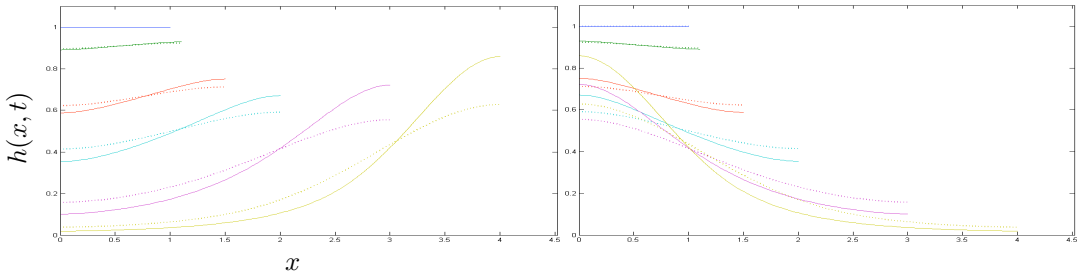

FIGURE 4. Numerical solutions to the unsteady problem with nonzero surface tension, for an initially-uniform sheet $h_i(x, 0) = 1$, with left-hand end fixed at $x = 0$ and right-hand end at $s(t) = 1+t$ (pulled at unit speed). The applied field is such that $R(x)$ (defined in (60)) takes values $R(x) = 1$ (left-hand figure) and $R(x) = -1$ (right-hand figure). The sheet profile $h(x, t)$ is shown at times $t = 0, 0.1, 0.5, 1, 2, 3$, for surface tension $\gamma = 1$ (solid) and $\gamma = 4$ (dashed).

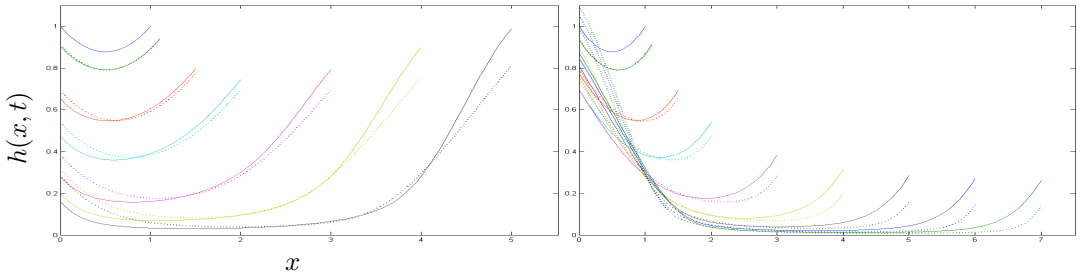

FIGURE 5. Evolution of a non-flat initial sheet (68) under the action of the electric field such that $R(x) = 1$ (left-hand plot; profile $h(x, t)$ shown at times $t = 0, 0.1, 0.5, 1, 2, 3, 4$) and $R(x) = -1$ (right-hand plot; profile $h(x, t)$ shown at times $t = 0, 0.1, 0.5, 1, 2, 3, 4, 5, 6$). Other details as for figure 4.

and nonzero surface tension cases, the general feature observed is that the sheet thins more rapidly as surface tension decreases. These observations suggest that

nonzero surface tension will delay the breakup of such sheets (though we are unable to carry our numerics through to breakup time).

The final example we consider is a more realistic externally-applied electric field, $\boldsymbol{E}_{ext}$, across an initially-uniform sheet. We use the external field given in (81) (Appendix B),

$$\boldsymbol{E}_{ext} = \hat{z}\boldsymbol{e}_x + x\boldsymbol{e}_{\hat{z}}, \tag{69}$$

where $\hat{z}$ is related to the dimensionless coordinate z (used from §2.2 onwards) by $\hat{z} = \delta z$ (it is the dimensionless but unstretched coordinate perpendicular to the sheet). The corresponding field within the sheet is

$$\boldsymbol{E} = a(x)\boldsymbol{e}_z + O(\delta), \tag{70}$$

where $a(x)$ is determined by solving (82) numerically. The function $a(x)$, together with its gradient, is shown in figure 6; it is very close to linear, but not quite. This function $a(x)$ is substituted in (42), which is then solved together with (43)

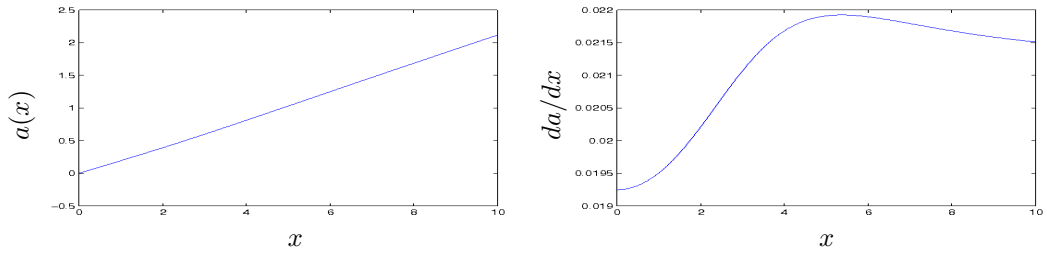

FIGURE 6. Electric field function $a(x)$ and its derivative.

subject to the boundary conditions. The results for the sheet evolution are shown in figures 7 (end velocity of sheet specified) and 8 (constant force prescribed at the sheet's end), for the two surface tension values $\gamma = 1, 4$.

5. Discussion and conclusions

We have used systematic asymptotic expansions to derive a new model for the dynamics of a thin film of nematic liquid crystal, under the action of stretching from its ends, and an externally-applied electric field. With certain simplifying assumptions (as outlined in §2), we deduce that (as for the Newtonian case) the sheet is flat to leading order, its centerline lying along the x-axis. The asymptotic analysis must be taken to second order in the film aspect ratio in order to obtain a closed system; when this is done two coupled PDEs are obtained for the sheet thickness $h(x,t)$, and the velocity of the sheet along its axis, $u(x,t)$. These PDEs depend also on the director angle θ which, with the same anchoring conditions on each free surface, is also a function only of the axial coordinate (and possibly time), $\theta(x,t)$, and this is determined by the anchoring conditions at the free surfaces of the sheet and by the externally-applied electric field, which can be

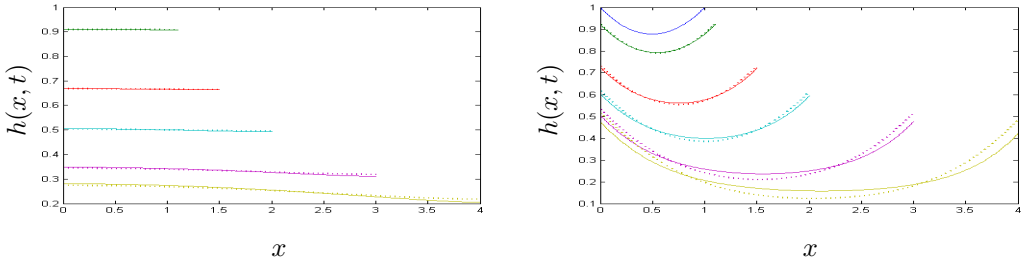

FIGURE 7. Numerical solutions to the unsteady problem with nonzero surface tension, for an initially-uniform sheet $h_i(x,0) = 1$ (left-hand figure) and non-flat initial condition (68) (right-hand figure). The left-hand end is fixed and its right-hand end is pulled at unit speed, so that its position is at $s(t) = 1 + t$. The applied field is given by (69), (70) ($a(x)$ as defined in (82) and plotted in Fig. 6). The sheet profile $h(x,t)$ at times $t = 0, 0.1, 0.5, 1, 2, 3$ is shown, for surface tension $\gamma = 1$ (solid) and $\gamma = 4$ (dashed).

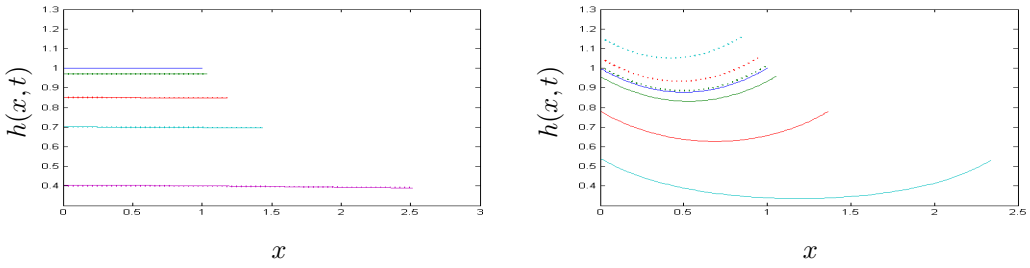

FIGURE 8. Numerical solutions to the unsteady problem with nonzero surface tension, for an initially-uniform sheet $h_i(x,0) = 1$ (left-hand figure, sheet profile shown at times $t = 0, 0.1, 0.5, 1, 2$) and non-flat initial condition (68) (right-hand figure, sheet profile shown at times $t = 0, 0.1, 0.5, 1$). The left-hand end is fixed while the right-hand end is pulled with a force of 1.8 units, and the applied field is as for Fig. 7. Surface tension values $\gamma = 1$ (solid) and $\gamma = 4$ (dashed) are shown.

solved for separately as explained in Appendix B. This calculation of the electric field is another contribution of this paper.

The full system, accounting for surface tension effects, the applied field, the surface anchoring of the nematic molecules, and suitable conditions at the sheet's ends, is summarized in §2.3. With no applied field, it is found that the evolution is exactly as for a Newtonian sheet, but the presence of an electric field gradient can dramatically change matters. An exact method for finding solutions (which follows the approach of Howell [10] for the Newtonian case) is presented for the zero surface tension case. When surface tension effects are significant numerical methods must be used, and several examples are presented for this case.

The analysis has several limitations, which a more in-depth (and considerably more complicated) analysis is required to resolve. Firstly, in order to solve

explicitly for the director angle, we only consider electric field effects that are subdominant to the internal elasticity of the sheet (though dominant over surface energy effects). Therefore, our analysis will be valid only for moderate applied electric fields. Secondly, motivated in part by our zero-field results, which reduced essentially to the model for the Newtonian sheet, we used a "Newtonian" simplification to reduce the governing equations in the applied-field case: that is, we set all the Leslie viscosities other than the Newtonian analog, α_4, to zero. We saw explicitly that this simplification is rigorously justifiable in the field-free case, but it is not obvious whether it is a legitimate simplification in the more general case with an applied field. This issue would benefit from further consideration, and in a future publication we will investigate very simple flows with an applied field and different (nonzero) Leslie viscosities.

Experiments on a similar setup (but with liquid crystalline fibers, rather than sheets, in extensional flow) have been carried out by Savage *et al.* [20]. Although Newtonian fibers in extension are governed by the same model as Newtonian sheets in extension (with a change only of Trouton ratio; the model is the same as the field-free case derived here), an extensional nematic fiber is quite different to an extensional nematic sheet, primarily because of the surface anchoring. With a nematic sheet, it is trivial for the director to adopt the same anchoring condition on each free surface (uniform director field throughout the sheet). However, for a circular fiber, any anchoring angle other than planar anchoring at the fiber surface leads to a nontrivial problem for the equilibrium director field within the fiber. Thus, the asymptotic analysis for an extensional nematic fiber will be much more complicated in general than the sheet considered here. These differences make it impossible to compare our results to those of [20].

Acknowledgements

LJC gratefully acknowledges financial support from the NSF on grant DMS 0908158, and the hospitality of the Centre de Recerca Matemàtica (CRM) during a month-long visiting Fellowship. TGM and LJC also gratefully acknowledge the support of this research through the Marie Curie International Reintegration Grant FP7-256417 *"Industrial Applications of Moving Boundary Problems"*, Ministerio de Ciencia e Innovación grant MTM2010-17162 and partial support by project 2009-SGR-345 from AGAUR-Generalitat de Catalunya. JL acknowledges support through a CRM Postdoctoral Fellowship.

Appendix A. Governing equation for general anchoring condition

$$\frac{F(\theta_B)}{G(\theta_B)}\left(h_0 u_0'(x)\right)_x + \frac{\gamma}{2} h_0 h_{0xxx} = 0 \tag{71}$$

where

$$G(\theta_B) = (\alpha_1 \cos(4\theta_B) - \alpha_1 + 2\cos(2\theta_B)(\alpha_2 + \alpha_3 - \alpha_5 + \alpha_6) + \tag{72}$$

$$+ 2\alpha_2 - 2\alpha_3 - 4\alpha_4 - 2\alpha_5 - 2\alpha_6) \tag{73}$$

$$F(\theta_B) = (2\cos(2\theta_B)(\alpha_1 + 2\alpha_4 + \alpha_5 + \alpha_6)(\alpha_2 + \alpha_3 - \alpha_5 + \alpha_6) + \tag{74}$$

$$+ \cos(4\theta_B)(\alpha_1(\alpha_2 - \alpha_3) + (\alpha_2 + \alpha_3)(\alpha_5 - \alpha_6)) + \tag{75}$$

$$+ \alpha_1\alpha_2 - \alpha_1\alpha_3 - 4\alpha_1\alpha_4 - 2\alpha_1\alpha_5 - 2\alpha_1\alpha_6 + \tag{76}$$

$$+ 4\alpha_2\alpha_4 + \alpha_2\alpha_5 + 3\alpha_2\alpha_6 - 4\alpha_3\alpha_4 - 3\alpha_3\alpha_5 - \alpha_3\alpha_6 - \tag{77}$$

$$-8\alpha_4^2 - 8\alpha_4\alpha_5 - 8\alpha_4\alpha_6 - 2\alpha_5^2 - 4\alpha_5\alpha_6 - 2\alpha_6^2) \tag{78}$$

Appendix B. The electric field within the sheet

The applied field satisfies Maxwell's equations both inside and outside the nematic sheet, with appropriate jump conditions at the interfaces. Within the sheet the slender scalings apply, with $x \sim L$, $z \sim \delta L$; and if $|\boldsymbol{E}| \sim E_0$ then the electric potential $\phi \sim \delta L E_0$. In dimensionless variables with these scalings then, the electric field within the sheet satisfies

$$\boldsymbol{E} = \nabla\phi = \delta\phi_x \boldsymbol{e}_x + \phi_z \boldsymbol{e}_z, \tag{79}$$

and, accounting for the dielectric anisotropy within the nematic, Maxwell's equations require $\nabla \cdot (\underline{\underline{\varepsilon}}\boldsymbol{E}) = 0$, so that

$$(\varepsilon_{33}\phi_z)_z + \delta(\varepsilon_{13}\phi_x)_z + \delta(\varepsilon_{13}\phi_z)_x + \delta^2(\varepsilon_{11}\phi_x)_x = 0$$

within the sheet. In this 2D case the coefficients of the dielectric tensor $\underline{\underline{\varepsilon}}$ can be written explicitly in terms of the director components $n_1 = \sin\theta$, $n_3 = \cos\theta$, as

$$\varepsilon_{33} = (\varepsilon_\parallel - \varepsilon_\perp)\cos^2\theta + \varepsilon_\perp,\ \varepsilon_{13} = (\varepsilon_\parallel - \varepsilon_\perp)\sin\theta\cos\theta,\ \varepsilon_{11} = (\varepsilon_\parallel - \varepsilon_\perp)\sin^2\theta + \varepsilon_\perp.$$

Since in the thin sheet approximation the director angle θ is independent of the coordinate z perpendicular to the film to leading order (see (23)), so that ε_{33} is independent of z, the leading-order electric potential ϕ_0 satisfies

$$\phi_0 = za(x) + b(x),$$

corresponding to an electric field (from (79))

$$\boldsymbol{E} = \phi_{0z}\boldsymbol{e}_z + O(\delta) = a(x)\boldsymbol{e}_z + O(\delta).$$

Here $a(x)$ is arbitrary, though in practice will have to match to a solution of Maxwell's equations outside the nematic sheet via the appropriate boundary conditions.

With the free energy density scaled with $K/(\delta^2 L^2)$, the dimensionless energy density W is then given by

$$2W = \theta_z^2 - \delta e(x)(\cos^2\theta + \lambda) + O(\delta^2),$$

where

$$e(x) = \frac{\delta L^2 E_0^2 \varepsilon_0 (\varepsilon_\parallel - \varepsilon_\perp)}{K} a(x)^2 = e_0 a(x)^2, \qquad \lambda = \frac{\varepsilon_\perp}{\varepsilon_\parallel - \varepsilon_\perp},$$

and $e(x)$ is assumed to be $O(1)$.

B.1. **The required exterior field.** The above relates to the electric field within the nematic sheet, but in practice we envisage an externally-supplied electric field, which we write in terms of (dimensionless) electric potentials ϕ (inside the film; see above) and Φ (outside the film); ϕ and Φ scale differently, as discussed below. Outside the nematic sheet we assume the dielectric tensor ε_{ij} to be the identity tensor δ_{ij}. Then, outside the sheet Φ satisfies Laplace's equation, and the jump conditions across the air-nematic interface are (in the dimensional, unscaled variables)

$$[\boldsymbol{\nu}^* \cdot \underline{\underline{\varepsilon}}^* \cdot \boldsymbol{E}^*] = 0, \quad [\boldsymbol{E}^* \cdot \boldsymbol{t}^*] = 0,$$

where $\boldsymbol{\nu}^*$ is the normal vector and $\boldsymbol{t}^*$ the tangent vector to the interface.

In the outer (air) region the geometry is no longer slender: both x^*- and z^*-coordinates scale with sheet length L^*, and we use dimensionless variables $(x, \hat{z})$ to denote this different scaling. We then have Laplace's equation in $(x, \hat{z})$ for the electric potential Φ (now made dimensionless by scaling with LE_0), and the above boundary conditions are applied, to leading order, on the line $\hat{z} = 0$. We only need consider Φ in the region $\hat{z} > 0$ since we know the sheet geometry is symmetric about the x-axis, to leading order. With our knowledge of the scalings and solution in the slender sheet region, the problem for the leading-order potential Φ_0 is then

$$\begin{aligned} \nabla^2 \Phi_0 &= 0 && \hat{z} > 0, \\ \Phi_{0x} &= 0 && \text{on } \hat{z} = 0, \\ \Phi_{0\hat{z}} = \varepsilon_{33}\phi_{0z} &= (\varepsilon_\parallel - \varepsilon_\perp)(\cos^2\theta + \lambda)a(x) && \text{on } \hat{z} = 0, \end{aligned}$$

where, recall, θ is a prescribed function of $a(x)$ given by (23). We solve this problem by writing $(\cos^2\theta + \lambda)a(x) = A'(x)$, and introducing a complex potential $f(Z)$, such that $\Phi_0 = \Re(f(Z))$, with $Z = x + i\hat{z}$. Then on the boundary $\hat{z} = 0$ we have $f'(Z) = \Phi_{0x} - i\Phi_{0\hat{z}} = -i\varepsilon_a A'(x)$, that is,

$$f'(Z) = -i\varepsilon_a A'(Z) \quad \text{on } \Im(Z) = 0$$

(here we have introduced the dielectric anisotropy, $\varepsilon_a = \varepsilon_\parallel - \varepsilon_\perp$). Provided $A'(Z)$ is analytic, this condition may then be analytically continued away from this boundary, and we may deduce that in fact

$$f(Z) = -i\varepsilon_a A(Z) + \kappa \quad \text{in } \Im(Z) > 0.$$

Hence we have the (leading order) electric potential and field everywhere; substituting for $\theta(x) = \theta_B g(a(x))$ from (23), we finally have

$$\boldsymbol{E}_{ext} = \nabla\Phi_0 = \varepsilon_a \left(\Im((\cos^2(\theta_B g(a(Z))) + \lambda)a(Z)), \Re((\cos^2(\theta_B g(a(Z))) + \lambda)a(Z))\right) + O(\delta), \tag{80}$$

with $g(a)$ given by (16). Thus, assuming that there is some way to generate the above exterior field for any given choice of $a(x)$, our original assumptions about the form of the electric field within the sheet are justified. For example, if we wish to consider a field $\boldsymbol{E} = a(x)\boldsymbol{e}_z + O(\delta)$ with $a(x) = x$, then the exterior field at any point $(x, \hat{z})$ outside the sheet must take the form

$$\boldsymbol{E}_{ext} = \varepsilon_a \left(\Im\left[(\cos^2\left(\frac{\theta_B E_a^2}{Z^2 + E_a^2}\right) + \lambda)Z\right], \Re\left[(\cos^2\left(\frac{\theta_B E_a^2}{Z^2 + E_a^2}\right) + \lambda)Z\right]\right) + O(\delta),$$

where we set $\alpha = 2$ in (16) for definiteness.

On the other hand, we can now turn the problem around and ask: for a given external field satisfying $\Phi_{0x}|_{\hat{z}=0} = 0$, what is the corresponding field within the nematic sheet? By way of illustration, suppose the external field is given by

$$\Phi_0 = \frac{1}{2}\Re(-iZ^2) = x\hat{z}, \quad \boldsymbol{E}_{ext} = \hat{z}\boldsymbol{e}_x + x\boldsymbol{e}_{\hat{z}}, \tag{81}$$

which satisfies the boundary condition. The function $A(Z)$ is then given by $A'(Z) = Z/\varepsilon_a$, so the (leading order) field within the sheet is $\boldsymbol{E} = a(x)\boldsymbol{e}_z$, where $a(x)$ satisfies

$$\frac{x}{\varepsilon_a} = a(x)\left[\cos^2\left(\frac{\theta_B E_a^2}{a(x)^2 + E_a^2}\right) + \lambda\right] \tag{82}$$

(again, we set $\alpha = 2$ in (16) for definiteness).

References

[1] Ben Amar, M., Cummings, L.J. *Fingering instabilities of driven thin nematic films.* Phys. Fluids **13** (2001), 1160–1166.

[2] Byrd, P.F., Friedman, M.D. *Handbook of elliptic integrals for engineers and physicists.* Springer-Verlag (1954).

[3] Chandrasekhar, S. *Liquid Crystals* (2nd Ed.) Cambridge University Press (1992).

[4] Cummings, L.J. *Evolution of a thin film of nematic liquid crystal with anisotropic surface energy.* Euro. Jnl. Appl. Math. **15** (2004), 651–677.

[5] Cummings, L.J., Kondic, L., Lin, T.-S. *Modeling and simulations of the spreading and destabilization of small nematic droplets.* Phys. Fluids, to appear (2011).

[6] Davidson, A.J., Mottram, N.J. *Flexoelectric switching in a bistable nematic device.* Phys. Rev. E **65** (2002), 051710.

[7] van de Fliert, B., Howell, P.D., Ockendon, J.R. *Pressure-driven flow of a thin viscous sheet.* J. Fluid Mech. **292** (1995), 359–376.

[8] De Gennes, P.G., Prost, J. *The Physics of Liquid Crystals* (2nd Ed.) International Series of Monographs on Physics (83) Oxford Science Publications

[9] Gradshteyn, I.S., Ryzhik, I.M. *Table of Integrals, Series and Products* (6th Edition). Academic Press, London (2000).

[10] Howell, P.D. *Extensional thin layer flows.* D.Phil thesis, University of Oxford (1994).

[11] Howell, P.D. *Models for thin viscous sheets.* Europ. J. Appl. Math. **7(4)** (1996), 321–343.

[12] Inoue, M., Yoshine, K., Moritake, H., Toda, K. *Evaluation of nematic liquid crystal director orientation using shear horizontal wave propagation.* J. Appl. Phys. **91** (2002), 2798–2802.

[13] Kneppe, H., Schneider, F., Sharma, N.K. *Rotational viscosity γ_1 of nematic liquid crystals.* J. Chem. Phys. **77(6)** (1982), 3203–3208.

[14] Leslie, F.M. *Theory of flow phenomena in liquid crystals.* Adv. Liquid Crystals **4** (1979), 1–81.

[15] Palffy-Muhoray, P. *The diverse world of liquid crystals.* Physics Today, September 2007.

[16] Poulard, C., Cazabat, A.-M. *Spontaneous spreading of nematic liquid crystals.* Langmuir **21** (2005), 6270–6276. (2005).

[17] Quintans-Carou, J., Duffy, B.R., Mottram, N.J., Wilson, S.K. *Shear-driven and pressure-driven flow of a nematic liquid crystal in a slowly-varying channel.* Phys. Fluids **18** (2006), 027105.

[18] Rapini, A., Papoular, M. *Distorsion d'une lamelle nématique sous champ magnetique. Conditions d'ancrage aux parois.* J. Phys. Colloq. C4 **30** (1969), 54–56.

[19] Rey, A.D., Cheong, A.-G. Texture dependence of capillary instabilities in nematic liquid crystalline fibres. Liquid Crystals **31**, 1271-1284 (2004).

[20] Savage, J.R., Caggioni, M., Spicer, P.T., Cohen, I. *Partial universality: pinch-off dynamics in fluids with smectic liquid crystalline order.* Soft Matter, **6** (1010), 892–895.

[21] Skarp, K., Lagerwall, S.T., Stebler, B. *Measurements of hydrodynamic parameters for nematic 5CB.* Mol. Crys. Liq. Cryst. **60** (1980), 215–236.

[22] Stewart, I.W. *The static and dynamic continuum theory of liquid crystals: A mathematical introduction.* Taylor & Francis, (2004).

[23] Tóth-Katona, T., Buka, A. *Nematic liquid crystal-air interface in a radial Hele-Shaw cell: Electric field effects.* Phys. Rev. E. **67** (2003), 041717.

[24] Ockendon, H., Ockendon, J.R. *Viscous flow. Cambridge University Press* (1995).

L.J. Cummings
Department of Mathematical Sciences
New Jersey Institute of Technology
Newark NJ 07102-1982

J. Low
Centre de Recerca Matemàtica
Campus de Bellaterra, Edifici C
08193 Bellaterra, Barcelona
Spain

T.G. Myers
Centre de Recerca Matemàtica
Campus de Bellaterra, Edifici C
08193 Bellaterra, Barcelona
Spain